

Seeded Porous Silicon Preparation as a Substrate in the Growth of ZnO Nanostructures

Kevin Alvin Eswar^{1, 2, 3, a*}, Ajis Lepit^{2, b}, Rosfayanti Rasmidi^{2, c},
Husairi Fadzilah Shuhaimi^{1, 3, d}, Nurul Afaah Abdullah^{1, 3, e},
Noor Aadilla Abdul Aziz^{1, 3, f}, Nur Amierah Mohd Asib^{1, 3, g}, Azlinda Aziz^{1, 2, 3, h},
Zuraida Khusaimi^{1, 3, i}, Salman A.H. Alrokayan^{5, j}, Haseeb A. Khan^{5, k},
Mohamad Rusop^{1, 4, l}, Saifollah Abdullah^{1, 3, m}

¹NANO-SciTech Centre (NST), Institute of Science, Universiti Teknologi MARA (UiTM),
40450 Shah Alam, Selangor, Malaysia

²Faculty of Applied Sciences, Universiti Teknologi MARA (UiTM), Cawangan Kota Kinabalu,
Sabah, Malaysia

³Faculty of Applied Sciences, Universiti Teknologi MARA (UiTM),
40450 Shah Alam, Selangor, Malaysia

⁴NANO-Electronic Centre (NET), Faculty of Electrical Engineering, Universiti Teknologi MARA
(UiTM), 40450 Shah Alam, Selangor, Malaysia

⁵Department of Biochemistry, College of Science, King Saud University (KSU), Riyadh 11451,
Kingdom of Saudi Arabia

^akevin.alvin86@gmail.com, ^bajis@sabah.uitm.edu.my, ^crosfa270@sabah.uitm.edu.my,
^dmhuseirifadzilah@yahoo.com, ^eafaahabdullah@yahoo.com, ^faadilaazizali@gmail.com,
^gamierahasib@yahoo.com, ^hazlindazz@gmail.com, ⁱzuraidakhusaimi@gmail.com,
^jhaseeb@ksu.edu.sa, ^kdr.salman@ksu.edu.sa, ^lrusop@salam.uitm.edu.my,
^msaifollah@salam.uitm.edu.my

Keywords: Porous Silicon, ZnO nanostructures, electrochemical etching, sol-gel, hydrothermal immersion, annealing temperature

Abstract. In this work, seeded porous silicon (PSi) was used as a substrate in the growth of ZnO nanostructures. PSi was prepared by electrochemical etching method. ZnO thin films as seeded were deposited via sol-gel spin coating method. ZnO nanostructures were grown on seeded PSi using hydrothermal immersion method. In order to study the effect of post-heat treatment on the substrate, post annealing temperature were varied in the range of 300 to 700 °C. The FESEM results shows ZnO thin film composed of nanoparticles were distributed over the PSi surface. Based on AFM characterization, the smoothest surface was produced at post annealing temperature of 500 °C. There are two different peaks appeared in PL characterization. The peak in near-UV range is belonging to ZnO thin films while a broad peak in visible range can be attributed to ZnO defects and PSi surface. In addition, FESEM, XRD and PL were used to characterize the ZnO nanostructures. The FESEM results revealed ZnO nano-flower were successfully grown on seeded PSi. Hexagonal wurtzite of ZnO with dominated by the plane (100), (002), and (101) was found by XRD characterization. Two different peaks in UV range and visible range can be attributed to ZnO nano-flower and various defects of ZnO, respectively.

Introduction

Special characteristic of a wide band gap of 3.37 eV and a large binding energy of 60 meV make ZnO semiconductor become a potential material in optoelectronic device applications. ZnO nanostructures doped by Aluminum were studied by Mamat et al. for ultraviolet photoconductive sensors [1]. Baek et al. have studied hybrid silicon wire and planar solar cells for solar cell application as a potential renewable energy source [2]. In addition, Kim et al. have proposed that the photoluminescence (PL) properties of ZnO nanostructures grown on PSi can be applied to white

light emitting devices [3]. Several methods have been used to produce ZnO nanostructures including radio frequency (RF) magnetron sputtering, pulsed laser deposition, chemical vapour deposition, atomic layer deposition, sol-gel deposition and hydrothermal immersion deposition [4-10]. Among them, hydrothermal immersion method was very popular due to simplicity, low cost and can be conducted in low-temperature. Self-assembly deposition such as hydrothermal immersion method need a nucleation site called seed layer or catalyst to produce high crystalline quality nanostructures [11]. In this work, ZnO thin films were deposited on PSi using spin coating method. Then, the ZnO nanostructures were grown on seeded PSi via hydrothermal immersion method.

Experimental

P-type silicon was cleaned using acetone, methanol and diluted hydrofluoric acid (HF) before being etched via electrochemical etching [12]. A mixture of HF 48% and absolute ethanol was used as an electrolyte. The etching process was assisted by current densities of 20 mA/cm^2 and potential difference of 100 V for 20 minutes. In order to prepare ZnO thin film as a seed layer on PSi, sol-gel spin coating was employed. Zinc acetate dihydrate, diethanolamine, and isopropyl were used as starting material, stabilizer and solvent, respectively. The rotation per minute (rpm) of spin-coater was maintained at 300 in 60 s [13]. The seeded PSi was treated in various annealing temperature in the range of 300 to 700 °C. Then, the sample was characterized using field emission scanning electron microscopy (FESEM), atomic force microscopy (AFM), and photoluminescence (PL) spectroscopy. ZnO nanostructures were grown on the selected seeded PSi substrate via hydrothermal immersion method. Zinc nitrate hexahydrate, hexamethylenetetramine (HMTA), and deionized water were used as a starting material, stabilizer and solvent respectively [14]. The surface morphology and the crystallinity were studied using FESEM, and X-ray diffraction (XRD) spectroscopy, respectively. The optical property was investigated using PL spectroscopy.

Result and discussion

Fig. 1 shows the FESEM and AFM images of seeded PSi that treated in different post-annealing temperatures. Based on the figure, the seeded PSi was composed by ZnO nanoparticles. The particle size of 24.7 nm increased to 25.6 nm when the annealing temperature was increased from 300 °C to 400 °C. This phenomena has also been observed by other researcher [15]. It can be explained by thermal expansion where the kinetic energy of an atom increases due to the increase of post-annealing temperatures. However, the average particle size decreased to 21.4 nm at annealing temperature of 500 °C. This can be explained by the re-arrangement of atom within the ZnO nanoparticles. The atom has sufficient thermal energy and can move to any space within the particle and crystalline arrangement. Therefore, the size of the particle decreases due to the ability to fill the space within the crystalline structure. It is believed that the crystalline quality has also increased because the atom will move to the most favourable position [16]. Furthermore, the atoms will move to adjacent particles at 600°C and 700 °C, therefore, they will merges together and subsequently form a larger particle. In addition, the increases of the annealing temperature were increased the thermal energy including the particle surface energy [17]. So, it was merged to adjacent particles to minimize the surface energy. The average surface roughness of seeded PSi was analysed by using AFM characterization instrument. The average surface roughness of ZnO thin film surface is 1.51 nm at annealing temperature of 300 °C and increases to 1.64 nm at 400 °C. However, the average surface roughness decreases to 1.47 nm at 500 °C. Then it becomes rougher once more when increasing the annealing temperatures. The average surface roughness of nanostructured film is increased at 400 °C due to non-uniformity of ZnO nanoparticles size. At annealing temperature of 500 °C, the crystalline quality increases due to the atom arrangements being in favourable position and therefore making the average surface roughness decrease [18]. Besides, the size of ZnO nanoparticles was more uniform at this annealing temperature as seen in FESEM images. The

average surface roughness increases when the post-annealing temperature was increased from 500 °C to 600 °C. This may be attributed to the non-uniform in the increases of ZnO nanoparticles size. The same phenomenon was also seen when the post-annealing temperature increased to 700 °C. As discussed before, the increment of ZnO nanoparticles may be related to the increases of its surface energy. It tends to merge with its adjacent particles to reduce the surface energy [19]. The non-uniform ZnO particles sizes contribute high average surface roughness.

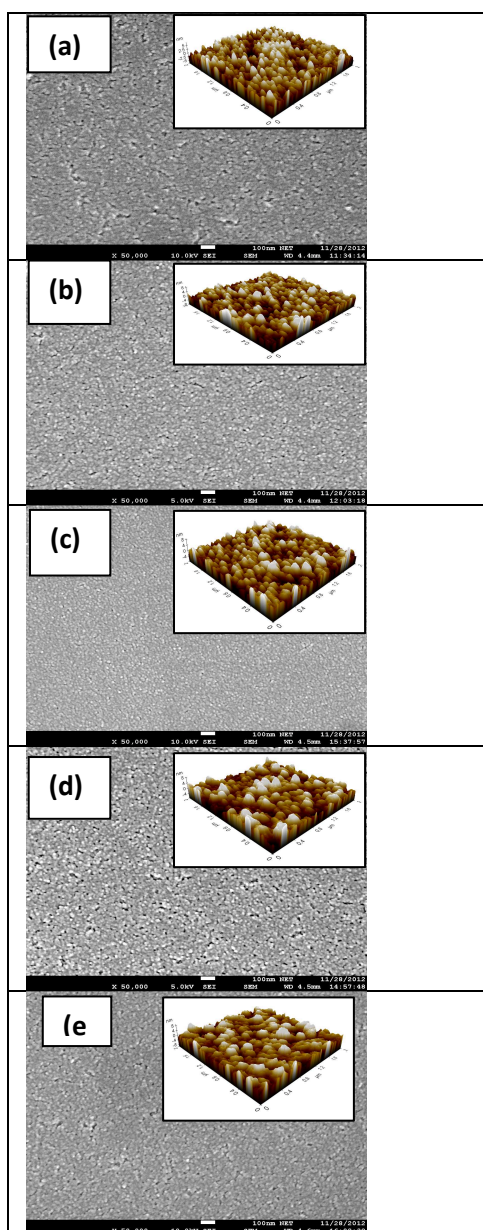


Fig. 1, FESEM images of nanostructured ZnO film deposited on PSi with post annealing of (a) 300 °C, (b) 400 °C, (c) 500 °C, (d) 600 °C and (e) 700 °C (The inserted picture is the AFM image)

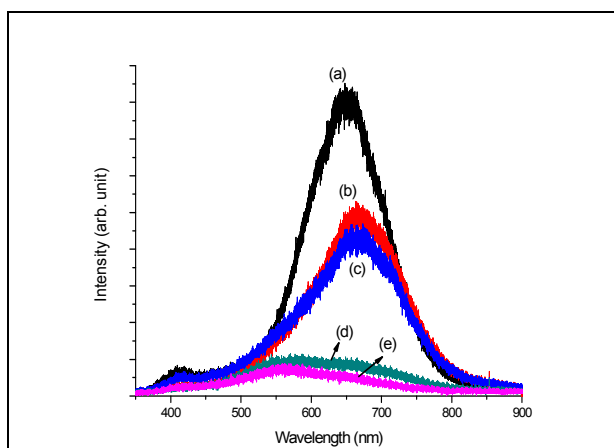


Fig. 2, PL spectra of nanostructured ZnO film in post annealing temperatures of (a) 300 °C, (b) 400 °C, (c) 500 °C, (d) 600 °C and (e) 700 °C

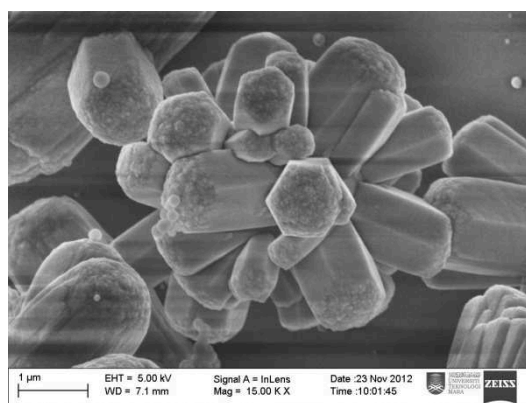


Fig. 3, The FESEM image of the ZnO nanostructures on the seeded PSi

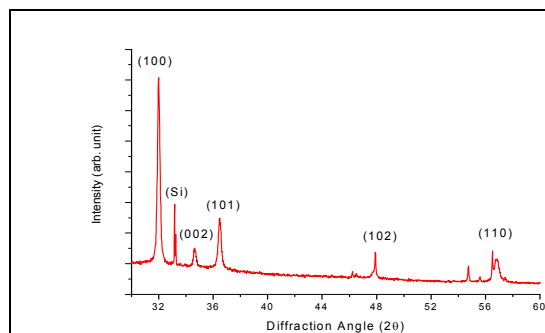


Fig. 4, The XRD pattern of ZnO nanostructures on seeded PSi

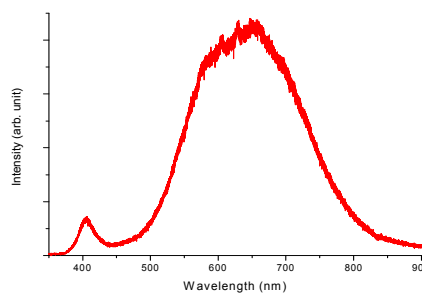


Fig. 5, The PL spectra of the ZnO nanostructures on seeded PSi

Fig. 2 shows the PL spectra of the seeded PSi in the range of 350 nm to 900 nm. In general, the findings show three distinct peaks at UV-blue region, green-yellow region and red region. The first peak, in UV-blue region is relates specifically to the ZnO nanoparticles; the second peak in green-yellow region is relevant to the defects of nanostructured ZnO film; and the third peak, within the red is due to the PSi surface [20]. Fig. 3 shows the FESEM images of the ZnO nanostructures on the seeded PSi template. Based on the figure, it was produced flower-like structures of ZnO. The petals were composed of ZnO nanorod with ZnO nanoparticles still can be seen on the top of it. XRD spectrometer was used to study the structural properties of ZnO nanostructures. Fig. 4 shows the XRD pattern of the ZnO nanostructures on seeded PSi. As can be seen, several diffraction peaks were observed in the range of 30° to 60° . It can be attributed to the presence of ZnO nanostructures and seeded PSi template. Peak of (100), (002), (101), (102) and (110) correspond to hexagonal ZnO wurtzite can be observed apparently (JCPDS No: 36-1451). Besides, peak of impurity corresponds to silicon was also appeared in between of plane (100) and (002), located at $\sim 33.2^\circ$ for all samples (JCPDS No: 17-0901) [21, 22]. Fig. 5 shows the PL spectra of ZnO nanostructures on seeded PSi in the range of 350 nm to 900 nm. As can be seen, two distinct peaks are appeared where low emission peak intensity located within UV region and high intensity within the visible region. In the UV region, it can be attributed to the intrinsic property of the wurtzite ZnO and excitonic recombination [23, 24]. On the other hand, the visible region can be ascribed to the radial recombination of photo-generated holes with single ionized charge states of specific defects, such as oxygen vacancies or zinc interstitials [25-27].

Conclusion

As a conclusion, the result revealed that the temperature is highly influenced the formation of ZnO thin films. Then, the ZnO nano-flower was successfully grown on seeded PSi. The XRD result shows the formation of hexagonal ZnO wurtzite. In PL spectra, two peaks are appeared in UV and visible region. It can be attributed to the excitonic recombination in the UV region and ZnO defects in the visible region.

Acknowledgement

We would like to express our gratitude to Ministry of Education Malaysia, Research Grant from the Ministry of Science, Technology and Innovation of Malaysia. This work was supported by the Long-Term Research Grant Scheme for Nanostructures, Nanomaterials and Devices for Fuel Cells and Hydrogen Production (600-RMI/LRGS 5/3 (3/2013)) and Research Management Institute (RMI), Universiti Teknologi MARA (UiTM), Malaysia for their support. The authors would also like to acknowledge the Department of Biochemistry, College of Science, King Saud University, Kingdom of Saudi Arabia for the Research Collaboration and Support.

References

- [1] Mamat M.H., Khusaimi Z., Zahidi M.M., and Mahmood M.R. Performance of an Ultraviolet Photoconductive Sensor Using Well-Aligned Aluminium-Doped Zinc-Oxide Nanorod Arrays Annealed in an Air and Oxygen Environment, *Japanese Journal of Applied Physics*, 50 (6) (2011) 06GF05.
- [2] Baek S.-H., Kim S.-B., Shin J.-K., and Hyun Kim J. Preparation of hybrid silicon wire and planar solar cells having ZnO antireflection coating by all-solution processes, *Solar Energy Materials and Solar Cells*, 96 (2012) 251-256.
- [3] Kim M.S., Yim K.G., Kim S., Nam G., and Leem J.-Y. White light emission from nano-fibrous ZnO thin films/porous silicon nanocomposite, *Journal of Sol-Gel Science and Technology*, 59 (2) (2011) 364-370.
- [4] Rouhi J., Alimanesh M., Mahmud S., Dalvand R.A., Raymond Ooi C.H., and Rusop M. A novel method for synthesis of well-aligned hexagonal cone-shaped ZnO nanostructures in field emission applications, *Materials Letters*, 125 (0) (2014) 147-150.
- [5] Rouhi J., Alimanesh M., Dalvand R., Ooi C.H.R., Mahmud S., and Mahmood M.R. Optical properties of well-aligned ZnO nanostructure arrays synthesized by an electric field-assisted aqueous solution method, *Ceramics International*, 40 (7, Part B) (2014) 11193-11198.
- [6] Rouhi J., Mahmud S., Naderi N., Ooi C.R., and Mahmood M.R. Physical properties of fish gelatin-based bio-nanocomposite films incorporated with ZnO nanorods, *Nanoscale Research Letters*, 8 (1) (2013) 1-6.
- [7] Cui L., Zhang H.-Y., Wang G.-G., Yang F.-X., Kuang X.-P., Sun R., and Han J.-C. Effect of annealing temperature and annealing atmosphere on the structure and optical properties of ZnO thin films on sapphire (0001) substrates by magnetron sputtering, *Applied Surface Science*, 258 (7) (2012) 2479-2485.
- [8] Lan S.M., Uen W.Y., Chan C.E., Chang K.J., Hung S.C., Li Z.Y., Yang T.N., Chiang C.C., Huang P.J., Yang M.D., Chi G.C., and Chang C.Y. Morphology and optical properties of zinc oxide thin films grown on Si (100) by metal-organic chemical vapor deposition, *Journal of Materials Science: Materials in Electronics*, 20 (S1) (2008) 441-445.
- [9] Eswar K.A., Rouhi J., Husairi F.S., Dalvand R., Alrokayan S.A.H., Khan H.A., Rusop Mahmood M., and Abdullah S. Hydrothermal growth of flower-like ZnO nanostructures on porous silicon substrate, *Journal of Molecular Structure*, 1074 (0) (2014) 140-143.
- [10] Eswar K.A., Azlinda A., Husairi F.S., Rusop M., and Abdullah S. Post Annealing Effect on Thin Film Composed ZnO Nano-particles on Porous Silicon, *Nano Bulletin*, 2 (2) (2013) 130212(1-6)
- [11] Ko Y.H., Leem J.W., and Yu J.S. Controllable synthesis of periodic flower-like ZnO nanostructures on Si subwavelength grating structures, *Nanotechnology*, 22 (20) (2011) 205604.
- [12] Eswar K., Azlinda A.A., Husairi F., Rusop M., and Abdullah S. Synthesis of ZnO Thin Film on Porous Silicon by Spin Coating in Various Low Molarities Precursor, *Advanced Materials Research*, 701 (2013) 167-171.
- [13] Eswar K.A., Ab Aziz A., Rusop Mahmood M., and Abdullah S. Surface Morphology of Seeded Nanostructured ZnO on Silicon by Sol-Gel Technique, *Advanced Materials Research*, 667 (2013) 265-271.
- [14] Eswar K.A., Husairi H.F., Rusop M., and Abdullah S. ZnO nanostructures on different silicon-based substrate via simple sol-gel immersion method, *Int. J. Microstructure and Materials Properties*, 8 (6) (2013) 478-487.
- [15] Varnamkhasti M.G., Fallah H.R., and Zadsar M. Effect of heat treatment on characteristics of nanocrystalline ZnO films by electron beam evaporation, *Vacuum*, 86 (7) (2012) 871-875.

-
- [16] Min S.K., Kwang G.Y., Jae-Young L., Soaram K., Giwoong N., Dong-Yul L., Jin S.K., and Jong S.K. Effects of Annealing Temperature on the Structural and the Optical Properties of ZnO Thin Films Grown on Porous Silicon by Using Plasma-assisted Molecular Beam Epitaxy, *Journal of the Korean Physical Society*, 59 (3) (2011) 2343.
- [17] Callister W.D., *Material Science And Engineering: An Introduction*, 7th ed.: John Wiley and Son (Asia) Pte. Ltd, 2007.
- [18] Eswar K.A., Rouhi J., Husairi H.F., Rusop M., and Abdullah S. Annealing Heat Treatment of ZnO Nanoparticles Grown on Porous Si Substrate Using Spin-Coating Method, *Advances in Materials Science and Engineering*, 2014 (2014) 6.
- [19] Neouze M.-A. Nanoparticle assemblies: main synthesis pathways and brief overview on some important applications, *Journal of Materials Science*, 48 (21) (2013) 7321-7349.
- [20] Huang X.L., Ma S.Y., Ma L.G., Bian H.Q., and Su C. Microstructure and optical properties of ZnO/porous silicon nanocomposite films, *Physica E: Low-dimensional Systems and Nanostructures*, 44 (1) (2011) 190-195.
- [21] Min S.K., Kwang G.Y., Jae-Young L., Soaram K., Giwoong N., Do Y.K., Sung-O K., Dong-Yul L., Jin S.K., and Jong S.K. Nanocrystalline ZnO Thin Films Grown on Porous Silicon by Sol-gel Method and Effects of Post-annealing, *Journal of the Korean Physical Society*, 59 (2) (2011) 346.
- [22] Hsu H.C., Cheng C.S., Chang C.C., Yang S., Chang C.S., and Hsieh W.F. Orientation-enhanced growth and optical properties of ZnO nanowires grown on porous silicon substrates, *Nanotechnology*, 16 (2) (2005) 297-301.
- [23] Abdulgafour H., Yam F., Hassan Z., Al-Heuseen K., and Jawad M. ZnO nanocoral reef grown on porous silicon substrates without catalyst, *Journal of Alloys and Compounds*, 509 (18) (2011) 5627-5630.
- [24] Gao X., Li X., and Yu W. Flowerlike ZnO nanostructures via hexamethylenetetramine-assisted thermolysis of zinc-ethylenediamine complex, *The Journal of Physical Chemistry B*, 109 (3) (2005) 1155-1161.
- [25] Egelhaaf H.-J. and Oelkrug D. Luminescence and nonradiative deactivation of excited states involving oxygen defect centers in polycrystalline ZnO, *Journal of crystal growth*, 161 (1) (1996) 190-194.
- [26] Vanheusden K., Warren W., Seager C., Tallant D., Voigt J., and Gnade B. Mechanisms behind green photoluminescence in ZnO phosphor powders, *Journal of Applied Physics*, 79 (10) (1996) 7983-7990.
- [27] Aguilar C.A., Haight R., Mavrokefalos A., Korgel B.A., and Chen S. Probing electronic properties of molecular engineered zinc oxide nanowires with photoelectron spectroscopy, *ACS nano*, 3 (10) (2009) 3057-3062.